

## Current density distribution mapping in polymer electrolyte membrane fuel cell

T. Sousa<sup>1</sup>, D.S. Falcão<sup>2</sup>, A.M.F. R. Pinto<sup>2</sup>, C. M. Rangel<sup>1</sup>

<sup>1</sup> LNEG / Fuel Cells and Hydrogen Unit Paço do Lumiar, 22 1649-038 Lisboa Portugal

email: tiago.sousa@lneg.pt; carmen.rangel@lneg.pt

<sup>2</sup>CEFT, Departamento de Eng. Química, Universidade do Porto, Faculdade de Engenharia,  
Rua Dr. Roberto Frias, 4200-465 Porto, Portugal

---

### Abstract

*A non-uniform utilization of the active area due to inhomogeneous current density distribution is one of the main factors for poor fuel cell performance. Furthermore, it leads to hot points which can be responsible for thermal stress in the membrane electrode assemble (MEA). Therefore, it became extremely important to have a consistent technic to visualize in real time the current density and temperature distribution on the active area. For this purpose a printed circuit board (current scan lin® form S++) was used to measure the current density and temperature distribution. With this equipment it was possible to generate high resolution counters for these two variables. With these results the effect on the current density distribution by different flow fields design, oxygen stoichiometry, and temperature were analysed. Besides, these results can be used to provide crucial data for simulation work, in particular for validation purpose.*

---

**Keywords:** : PEMFC; current density distribution; segmented

### 1 Introduction

One of the milestones of any fuel cell design and development process is to guarantee an even current density distribution over the active area. When this objective is achieved the fuel cell operation is more efficient, which is extremely important because it can lead to low catalyst and reactants utilization. The main factor that contributes to an even distribution of current is a correct and suitable species transport, mainly in the flow channels. Poor flow channels and manifolds design can be responsible for preferential flow paths, dehumidification, and flooding; all these phenomena lead to an incorrect use of the active area. In addition, inadequate operation conditions such as species relative humidity, flow rate, pressure and temperature can also be responsible for poor use of the active area. In summary, an uneven electrochemical response of the active area is caused by complex interactions between design, operation parameters and materials properties.

To analyse all these factors several diagnostic techniques have been used; however, in the last decade segmented polymer electrolyte membrane fuel cell (SPEMFC) proved to be an excellent *in situ* diagnostic tool [1]. There are three categories of SPEMFC techniques: printed circuit board (PCB), resistors network and hall effect sensors; this paper

is dedicated to PCB, for more details about the other techniques reference [1] should be consulted.

Cleghorn et al. [2] developed one of the first techniques of measuring current distribution with a PCB in 1997 at Los Alamos National Laboratory. In this pioneer work they replaced the flow field on the anode side of a single PEMFC by a PCB. The anode gas diffusion layer was segmented by cutting silicone gasket material into a grid structure, with the cut-out areas filled with gas diffusion backing to match the pattern of the gold plated segments of the current collector plate. After this first work, several research groups have adopted this or very similar technique to map the current density; a good collection of the majority of these works can be found in reference [1]. Nowadays, the company S++<sup>®</sup> (Germany) [3] offers several solutions for the current density measurement in fuel cells, based on the PCB method. In our labs we have the “current scan lin” system provided by S++<sup>®</sup>. This system allowed us to measure the current density and temperature over an active area of 25 cm<sup>2</sup>. In this paper is presented the results obtained when this technique was used to investigate the effect of some key parameters on current distribution.

## 2 Experimental

### 2.1 Current density measurement

To map the current density it was used *current scan lin* provided by S++<sup>®</sup>. The MEA was sandwiched between two bipolar plates and the sensor plate was placed between the bipolar plate and the end plate on the cathode side. The sensor plate, with 49 gold segments of 25 mm<sup>2</sup>, was connected to the USB device, which allowed the signal to be transferred to the computer. The end plates were equipped with 4 heaters each, which delivered a heating power of approximately 24 watts per side. Figure 1 shows a schematic representation of the apparatus used to measure the current.

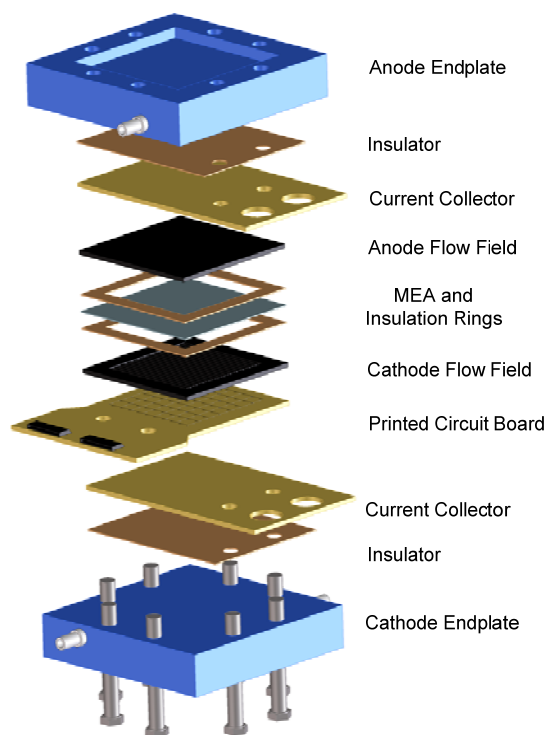


**Fig. 1 Exploded view of the segmented fuel cell used in this work.**

The current density was measured at each segment, and the measurement principle was based upon the dependence of the permeability of a magnetically soft material on the magnetization and temperature. Details about the physical principle go beyond the topic of this paper, therefore for more details reference [3] should be consulted. The segmentation was numbered from the inlet to the outlet on the basis of the cathode flow (Fig. 2).

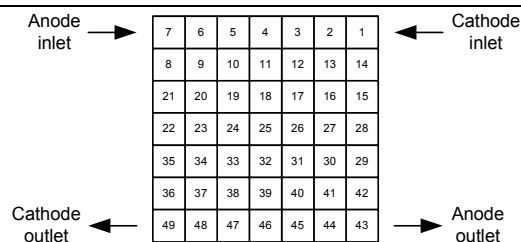


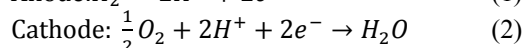
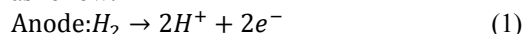
**Fig. 2 Segment position of measurement cell**

### 2.2 MEA preparation

To perform this work it was used one MEA provided by Lynntech Inc. The catalyst inks were brushed on to the electrolyte (Nafion 117<sup>®</sup>) at a loading of 2 mg cm<sup>-2</sup> PtRu for the anode side and 2 mg cm<sup>-2</sup> Pt Black for the cathode side. The gas diffusion layers (GDLs) were provided by Electrochem Inc. They were made out of carbon paper TGP-H-060 (Toray) which was treated in order to become hydrophobic. This treatment prevented the GDLs from becoming saturated by liquid water, while still allowing reactant gas and water vapour to pass through the pores of the material. The normal loading for treated material was 30wt% Teflon<sup>™</sup>. The active area of the MEA was 25 cm<sup>2</sup>.

### 2.3 Operational conditions

In this first effort to work with the segmented fuel cell it was used hydrogen as fuel and pure oxygen as oxidant. Therefore, the half-cell reactions were as follow:



For the basic operation conditions it was selected the stoichiometric factors ( $\lambda$ ) of 1.5 for the anode and 2 for the cathode. There are two main advantages of using  $\lambda > 1$ : water can be removed easily by the excess of gas flow; and higher flow rates keep the reactants concentration higher in the active area. Both hydrogen and oxygen were supplied with 100% of relative humidity, this way we guaranteed that the membrane remained well hydrated. The operational temperature was 40 °C and the operational pressure was 1 atm. The fuel cell was connected to an external loading in order to manipulate the total current drawn by the cell. Unless otherwise specified these were the basic operational conditions. As flow field it was used graphite plates with parallel topology. The channels dimensions were: 1 mm depth, 1 mm width and 46 mm length.

## 3 Results

### 3.1 Effect of current loaded on the cell

The total current loaded on the single cell equipped with parallel flow fields was varied between three values: 1 A, 2 A and 4 A. The current distribution obtained for each case is shown in Fig. 3. In addition to the current distribution the cell potential and the open circuit potential (OCP) were also measured. These results are shown in Table 1.

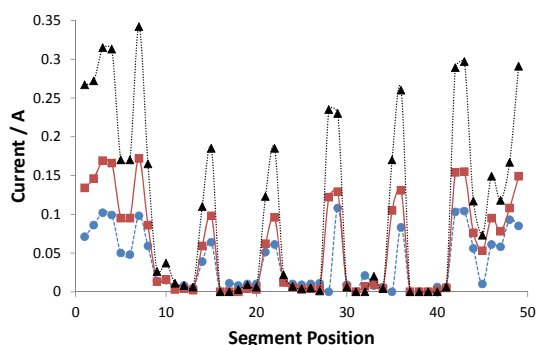


**Fig. 3 Current distribution at different current loads.** ● 1 A; ■ 2 A; ▲ 4 A.

As expected the cell potential decreased as the total current increased. However, the current distribution it was not homogenous over the active area. Even at low currents (1 A) was possible to observe periodic drops. With the increase of current this fluctuation became more evident. The highest current values were registered by the segments located on the borders of the active area. At the centre of the cell the current generation was almost zero. Fig. 4 shows a surface plot of the current as a function of the x y position at 4 A. This figure shows clearly that current was not generated at the centre of the cell. This behaviour led to a reduction of the overall cell performance because only 50% of the active area was used efficiently.

**Table 1 Cell potential at different current loads.**

Current / A	Potential / V
0	1.02 (OCP)
1	0.79
2	0.68
4	0.43

From the results observed in Figs. 3 and 4 could be concluded that the flow channels did not distribute the reactants evenly. Therefore, this phenomenon could be related to the flow channels configuration. It is well known that parallel flow fields could lead to preferential flow paths, i.e. there are channels with higher flow rate than others. As a consequence of this, the regions under the channels with low flow rate have a lack of reactants. To investigate if

this was the cause of the results discussed previously a simple 3D model was developed to analyse the gas velocity in the cathode channels. In this model was simply used the Navier-Stokes equation to calculate the velocity and pressure profile.

$$-\nabla p + \mu \nabla^2 \mathbf{v} + \rho \mathbf{g} = 0 \quad (1)$$

Where,  $\mathbf{v}$  is the velocity vector,  $p$  is the pressure,  $\mu$  is the viscosity,  $\rho$  is the density and  $\mathbf{g}$  is the gravity vector. To solve equation 1 was necessary to employ boundary conditions. Therefore, mass flow rate was set at the inlet and pressure at the outlet. To solve this simple problem COMSOL Multiphysics version 4.2 was used.

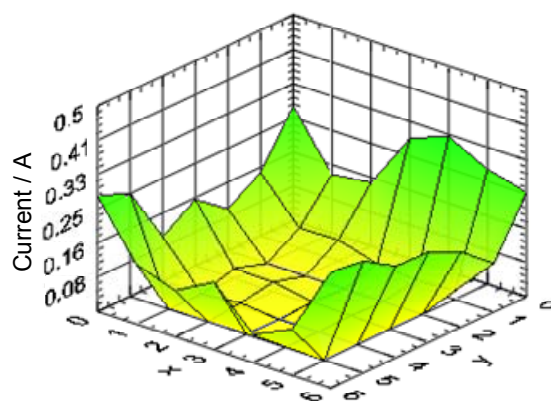


**Fig. 4 Surface plot of the current at 4 A. The cathode inlet was located at (6,0) and the outlet was located at (0,6).**

Fig. 5 shows the velocity profile predicted by the model for the cathode gas channels. From this figure it is possible to see huge velocity differences between the channels. The velocity reached the highest values in the manifolds, in particular near the inlet and outlet. In the central channels the velocity was very low, approaching  $0 \text{ m s}^{-1}$ , on the other hand, it is possible to see a slight velocity increase in the channels close to the inlet and outlet. To better visualise this phenomenon the velocity average in each channel was plotted in Fig. 6.

The non-homogeneous velocity distribution can be clearly seen in Fig 6. Velocity reached the highest value,  $0.53 \text{ ms}^{-1}$ , in the channel closest to the outlet (channel 1) followed closely by the channel near the inlet,  $0.49 \text{ ms}^{-1}$ . The lowest value,  $0.08 \text{ ms}^{-1}$ , was predicted to the central channels. These results explain the current distribution obtained by the segmented PCB. With this flow field configuration the central regions of the active area were not well reached by oxygen, therefore the electrochemical reaction could not occur efficiently. Several problems can arise due to this occurrence, beside the decrease of the overall efficiency, hot spots can emerge leading to thermal

stresses and the membrane can dehydrate under the regions with low gas flow rate.

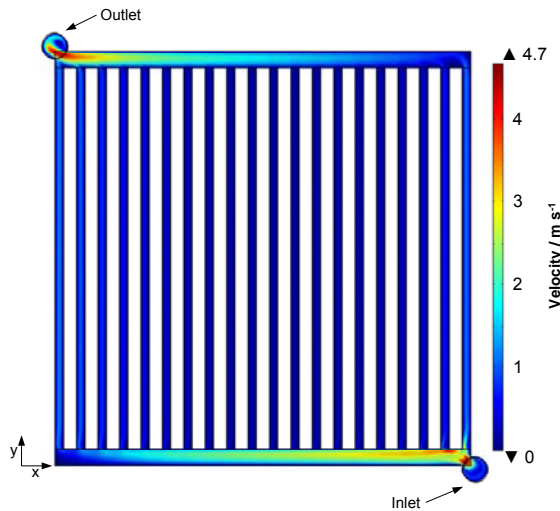


**Fig. 5** Velocity profile of oxygen at 40 °C and atmospheric pressure (plane at  $z = 0.5$  mm, half of the channel depth).

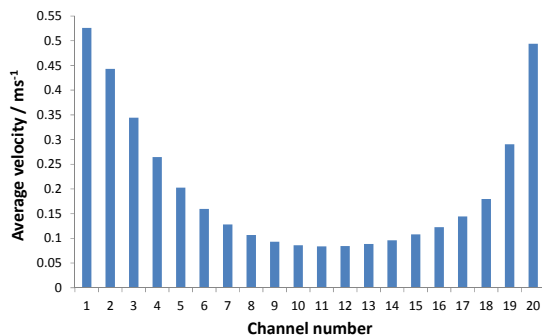


**Fig. 6** Oxygen average velocity in the channels.

### 3.2 Effect of temperature and flow rate.

The operational temperature is one of the most important operational parameters because it affects performance in two different ways: (1) as the temperature increases the exchange current density increases exponentially, (2) temperature variation affects all transport parameters, in particular mass transport coefficient increases significantly with temperature. Therefore, performance usually improves with elevated temperature [4].

In this study the cell temperature was varied to analyse the impact on current distribution. Three different cell temperatures were used (30, 40 and 50 °C), and the current load was kept at 4 A. Fig 7 shows the obtained results.

The cell potential measured for each temperature was very similar, around 0.4 V, this means that performance did not improved with temperature in this particular case. This conclusion can be

confirmed by analysing Fig. 7. As is possible to see the current distribution was very similar when temperature varied. Nevertheless, it is possible to observe performance improvement in the last segment (segment 49, near the cathode outlet) at 50 °C. This fact can indicate that at lower temperatures flooding can occur due to water accumulation in this region. At higher temperatures water can be vaporised easily, besides a slight velocity increase at the outlet was predicted by the model as the temperature increased. The average exit velocity was  $0.85 \text{ ms}^{-1}$  at 30 °C and  $0.92 \text{ ms}^{-1}$  at 50 °C. This is a very small difference (caused by changes on the viscosity and density) but still contributes to increase the blown effect.

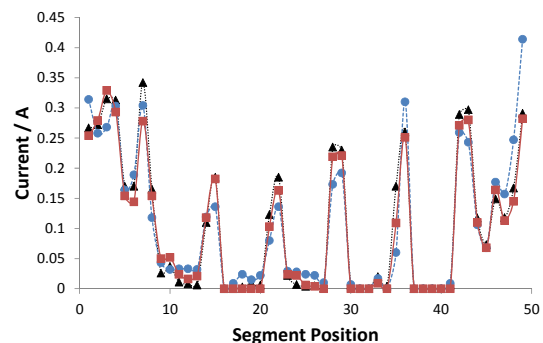


**Fig. 7** Current distribution at different temperatures with a load of 4 A. ■ 30 °C; ▲ 40 °C; ● 50 °C.

A fuel cell only works efficiently if the reactants flow rates at the inlets are equal or higher than the rate at which those reactants are being consumed. The ratio between the actual flow rate of a reactant at the inlet and the consumption rate of that reactant is called the stoichiometric ratio,  $\lambda$ . In general performance improves as the flow rate increases; for pure hydrogen  $\lambda$  should be between 1 and 1.2 and oxygen  $\lambda$  should be around 2[4].

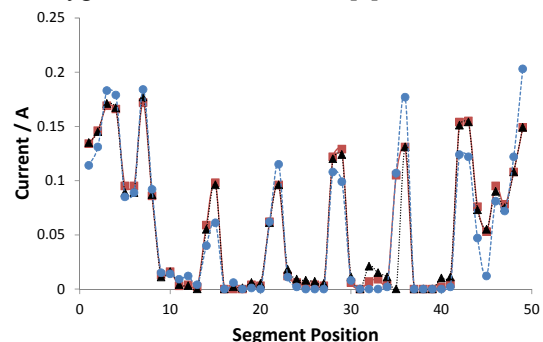


**Fig. 8** Current distribution at different flow rates with a load of 2 A. ■  $\lambda_{O_2}=1, \lambda_{H_2}=1$ ; ▲  $\lambda_{O_2}=2, \lambda_{H_2}=1.5$ ; ●  $\lambda_{O_2}=3, \lambda_{H_2}=2$ .

In this study three different stoichiometric ratio combinations were used: (1)  $\lambda_{O_2} = 1, \lambda_{H_2} = 1$ ; (2)  $\lambda_{O_2} = 2, \lambda_{H_2} = 1.5$  (3)  $\lambda_{O_2} = 3, \lambda_{H_2} = 2$ . Fig. 8 shows the results obtained for these three situations when a current load of 2 A was applied.

From these results it is possible to see that the overall current distribution was very similar, this means that increasing the stoichiometric ratio in this particular case did not have a big impact on performance. It is also interesting to notice that the curves trend in Fig. 8 is very similar to Fig. 9. With the highest flow rate, the current registered by the last segment had a significant increase when compared with the other situations. Behind this fact could be water management issues, just like discussed previously when temperature change was analysed.

### 3.3 Effect of flow field topology

To analyse how the flow field topology is important to the overall cell performance and in particular to the current distribution, the flow fields were changed to a five line serpentine provided by S++. Each channel was 0.7 mm depth and 0.7 mm width; the ribs between channels were 0.7 mm width. All other operational conditions were maintained constant.

Fig. 9 shows the current distribution for the two different flow fields when a total load of 4 A was applied. As is possible to see there is a massive difference; when the serpentine flow field was used the current distribution was much more homogeneous. This observation can be better understood by analysing Fig. 10. In this figure a surface plot of the current as a function of the x y position is shown. From the comparison of Fig. 10 and Fig. 4 it becomes clear the impact that inadequate flow fields can have on performance, in this particular case with the serpentine flow field the cell potential was 0.61 V, which corresponded to an increase of 30% on performance.

Fig. 9 also shows some oscillations on the current density distribution when serpentine flow field was used. These kind of fluctuation was also observed by Park et al. [5]. They related this behaviour to change of flow direction in the U bends regions. In these regions the gas flow must inverse direction; the result is a velocity drop, which could lead to an increase of mass transport loose. With the results obtained in this study the corner effect could not be verified; probability due to the phenomenon of current spreading. In future studies this effect should be forward analysed, for that the flow field must be segmented and its topology should maximise the corner flow effect.

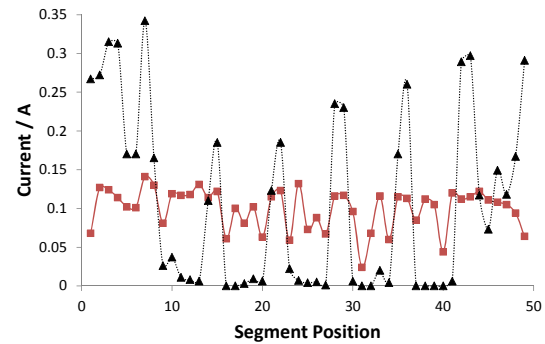


Fig. 9 Current distribution at 4 A and different flow fields. ■ serpentine; ▲ parallel.

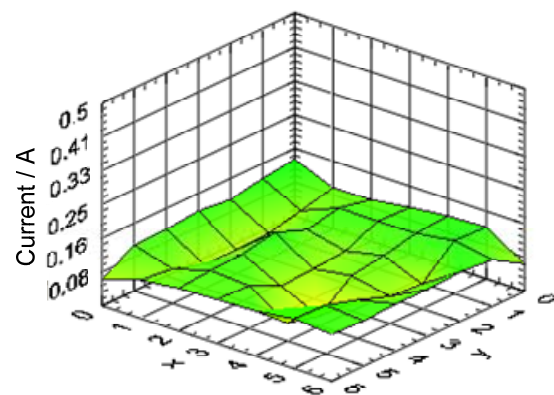


Fig. 10 Surface plot of the current distribution at 4 A for a single cell equipped with serpentine flow field. The cathode inlet was located at (6,0) and the outlet was located at (0,6).

## 4 Conclusions

In this study the influence of several operational parameters on the current distribution has been analysed. To map the current distribution it was used a printed circuit board, which was in contact with the cathode flow field. The main objective of this work was to test this equipment in order to obtain knowhow to develop more complex studies in the future.

From the obtained results became clear the impact that flow field design had on performance. An inadequate topology choice can lead to serious problems which can damage the electrolyte irreversibly. The serpentine flow field showed much better results than the parallel flow field; the current distribution was much more homogenous and the potential loss were much smaller. Besides, the parallel flow field showed problems with water management, especially at low temperatures and low flow rates.

The technique proved to be very reliable however it was noticed a main drawback: since none of the fuel cell components, i.e. the bipolar

since none of the fuel cell components, i.e. the bipolar plate, were segmented, it is possible that measurement errors occur due to the phenomenon of current spreading, which needs to be avoided so that the total current measured in each segment is not influenced by adjacent areas.

## 5 References

- [1] L.C. Pérez, L. Brandão, J.M. Sousa, A. Mendes, *Renewable and Sustainable Energy Reviews* 15 (2011) 169-185.
- [2] S.J.C. Cleghorn, C.R. Derouin, M.S. Wilson, S. Gottesfeld, *Journal of Applied Electrochemistry* 28 (1998) 663-672.
- [3] S++ Simulation Services, (2011).
- [4] F. Barbir, *PEM Fuel Cells : Theory and Practice*, Oxford Academic, 2005.
- [5] S.-M. Park, S.-K. Kim, S. Lim, D.-H. Jung, D.-H. Peck, W.H. Hong, *Journal of Power Sources* 194 (2009) 818-823.